Antarctic Science 1 (2): 169–178 (1989)

Low-level wind profiles at an Antarctic coastal station

J.C. KING

British Antarctic Survey, Natural Environment Research Council, High Cross, Madingley Road, Cambridge CB3 0ET, UK

Abstract: Wind and temperature profiles in the lowest 2000 m of the atmosphere at Halley (75°35'S, 26°50'W) have been analysed. Surface winds blow most frequently from the sector 090° ± 45° but the 2000 m wind direction is much more evenly distributed and appears to be determined by synoptic-scale pressure gradients. A simple one-dimensional boundary layer model, which includes the effects of stably-stratified air overlying a sloping surface, is able to reproduce some of the features of the observed profiles.

Received 24 February 1989, accepted 30 March 1989

Key words: aerology, atmospheric boundary layer, katabatic wind, meteorology.

Introduction

Surface winds over the Antarctic continent have long been noted for their high directional constancy and high mean speeds. Such observations suggest that the surface wind field is a result of stably-stratified air in the lower atmosphere overlying a sloping ice surface and that synoptic-scale pressure gradients play a secondary role in determining the surface wind (Ball 1960, Schwerdtfeger & Mahrt 1970, Parish 1980). These buoyancy-driven flows fall into two categories: the 'strong katabatic' winds seen in regions of large topographic slope, such as the coast of Adélie Land (Ball 1960), and the 'sloped inversion' winds (Schwerdtfeger & Mahrt 1970) prevalent over the gentler slopes of the continental interior. In the former case, the fundamental balance is between the downslope pressure gradient and frictional forces and the flow is directed more or less down the fall line. In the latter case, the flow is a result of near geostrophic balance between the downslope pressure gradient and Coriolis force, with friction playing a secondary role, and the flow makes a large angle with the fall line.

The surface wind at Antarctic coastal stations is influenced by synoptic-scale cyclones which move around the continent but do not appear to penetrate far inland (Parish 1980). In regions such as Adélie Land, where the steep slopes extend to the coast, the effects of topographic forcing are also reflected in the wind regime at coastal stations. In this paper we examine the low-level wind regime of a station separated from the steep continental slope by a gently-sloping ice shelf.

Halley station (75°35'S, 26°50'W) is situated towards the seaward edge of the Brunt Ice Shelf, Coats Land. The general location of the station is shown on Fig. 1 and a map showing the local topography in some detail is shown in Fig. 2. The ice front is marked by 30 m high ice cliffs; from here the surface of the ice shelf rises gently to the Hinge Zone, a disturbed region where the ice shelf meets the Caird Coast. Inland of the Hinge Zone, the land rises steeply to the continental plateau. The surface of the ice shelf is fairly uniform and, at Halley, is characterized by small sastrugi. Undulations, with a wavelength of about 1 km, run parallel with the Hinge Line and reach 5 m amplitude as the Hinge Zone is approached (Thomas 1973). The Hinge Zone itself is marked by very disturbed and crevassed ice.

Halley lies to the south of the main mid-latitude cyclone track but a significant number of cyclones do cross the

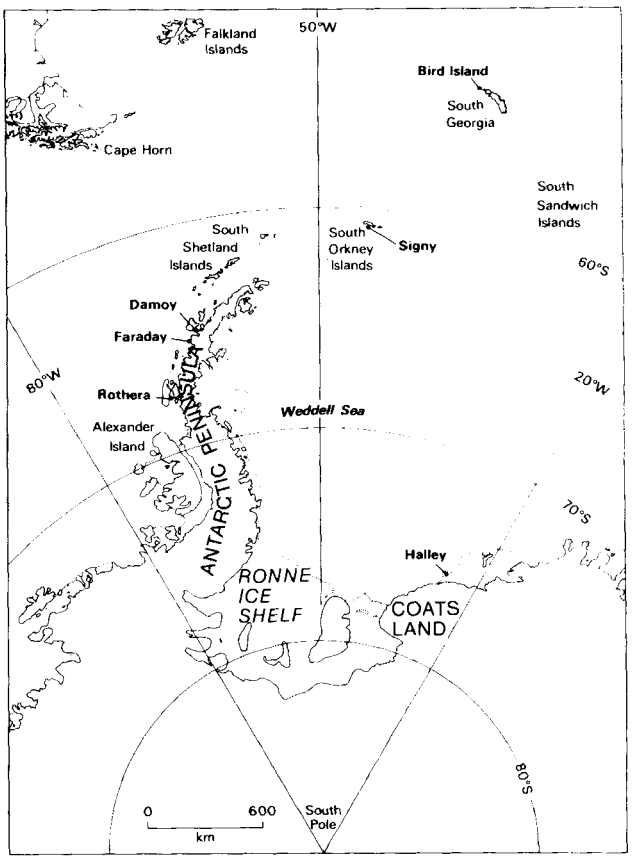


Fig. 1. A location map showing some of the places mentioned in the text.

https://doi.org/10.1017/S095410208900026X Published online by Cambridge University Press

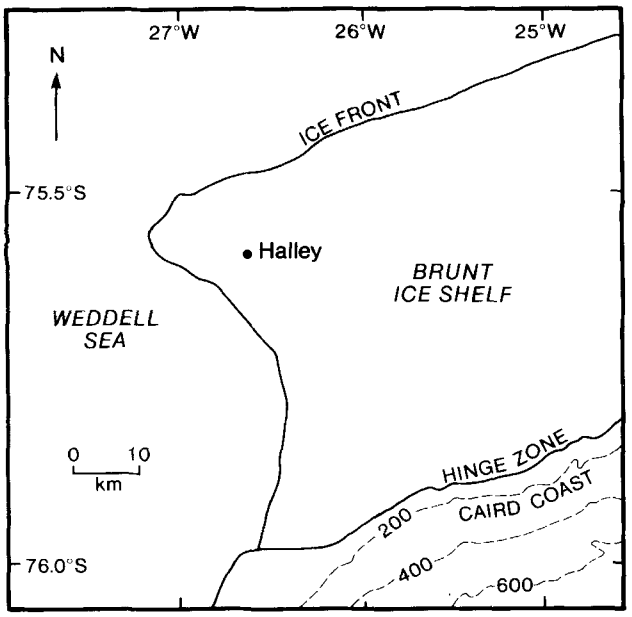


Fig. 2. A sketch map of the Brunt Ice Shelf in the region of Halley station. Approximate contours in metres, from Thomas (1973).

Antarctic Peninsula and track far enough south to affect conditions at Halley. Being south of the circumpolar trough, the mean synoptic pressure gradient forces an easterly flow. Occasional intense coastal cyclones can generate very strong winds and there is evidence (Astapenko 1964, Kottmeier 1986) that some cyclones penetrate inland along this sector of the Antarctic coast.

Observations

Surface and upper-air observations have been made at Halley since the station was established in 1957. In 1984, a Vaisala micro-CORA automated sounding system was installed. Regular upper-air soundings are made daily at 1200 GMT using Vaisala RS-80 radiosondes which measure pressure (P) using an aneroid capsule, temperature (T) using a bead thermistor and humidity (U) with a polymer capacitative sensor. Wind-finding is accomplished using the OMEGA very low frequency radio navigation aid. The sondes are suspended from 700 g hydrogen-filled balloons and ascend at about 4.5 ms^{-1} on release.

The sonde transmits a complete cycle of PTU measurements every 1–2 s and continuously relays phase information from the OMEGA stations being received. The micro-CORA ground station computes PTU values and wind components at 10-s intervals. This interval is commensurate with the smoothing applied to PTU values (both as a result of sensor response time and subsequent processing), but is much shorter than the averaging period applied to the OMEGA signals to extract wind information. OMEGA phases are calculated at 10 s intervals but are too 'noisy' to derive sensible winds from 10 s phase derivatives. Instead, phase derivatives are calculated by fitting a regression line to a 4-min series of phase values. The winds so derived are thus highly smoothed and are best regarded as averages over layers approximately 500 m deep. The wind values reported at launch time are taken from a surface observation (i.e. 10 m height above ground level) made at this time and the winds reported during the first 2 min of the sounding are simply an interpolation between this surface value and the computed 2-min wind.

Problems have been experienced with the OMEGA wind-finding system at Halley (S.P. Gill & D.W.S. Limbert, personal communication 1987). Only four of the eight OMEGA transmitters are reliably received. During the months September–December disturbed propagation conditions can lead to very large errors in the derived winds and few reliable wind soundings are available for the months of October and November.

During 1985, the 10 s PTU and wind data from the first 10 min (about 2500 m) of each daily sounding were recorded on microcomputer floppy disc. An assessment of the quality of the computed winds was made for each sounding, based on a knowledge of the behaviour of the OMEGA signals, and suspect wind soundings were rejected. The remainder were transferred to a mainframe computer for analysis.

Profile characteristics

Fig. 3 is a time–height plot of the monthly means of the northerly and easterly wind components and of potential temperature in the lowest 2000 m during 1985. For reasons discussed above, wind profiles for September through to November have been omitted.

The mean flow at the surface always has an easterly component. From January through to March, westerlies are seen above 1500 m, but during the winter months, April–August, the mean flow is easterly up to at least 2000 m. During these months there is an easterly wind maximum of about 6 ms^{-1}, centred at around 500 m. The mean northerly wind component is somewhat weaker. At the surface, the mean flow is southerly, but northerly flow predominates at higher levels. The northerly wind maximum seen during August may not be genuine since OMEGA propagation errors tend to generate a spurious northerly component which could be affecting some of the August soundings despite careful quality control.

The potential temperature profiles (Fig. 3c) show that the atmosphere is stably-stratified up to at least 2000 m throughout the year. The stratification is strongest during the winter months and the annual cycle is most marked at the lowest levels, as would be expected in response to the annual cycle of surface heating and cooling.

Wind roses for the surface and nominal levels of 500 m, 1000 m, 1500 m and 2000 m are shown in Fig. 4. These are

https://doi.org/10.1017/S095410208900026X Published online by Cambridge University Press

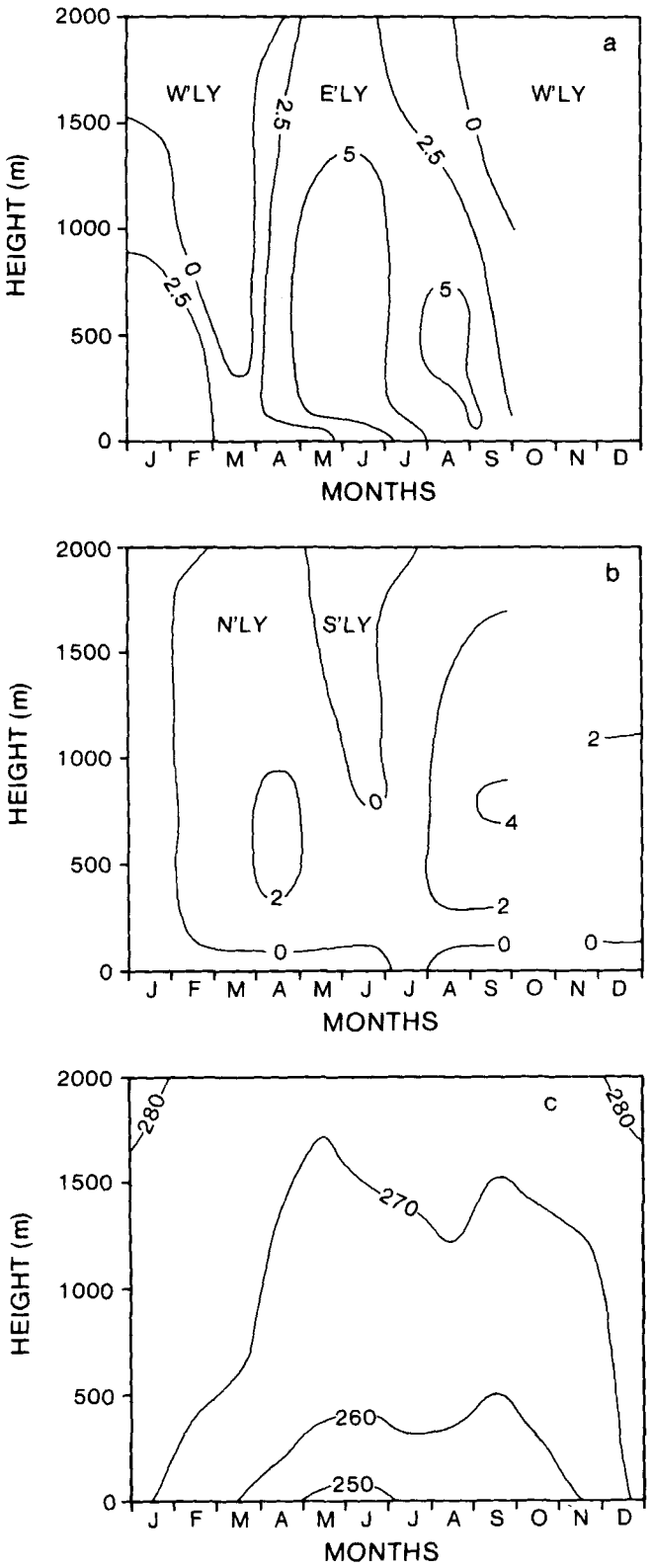


Fig. 3. Time–height contour plots of **a.** easterly wind component (ms^{-1}), **b.** northerly wind component (ms^{-1}) and **c.** potential temperature (K), based on monthly mean profiles for 1985.

based on all validated soundings since there are insufficient data available to look for seasonal variations. Surface winds are predominantly from the sector 090° ± 22°30' and this is the only sector in which strong (> 10 ms^{-1}) winds are observed. Winds from the south-westerly quadrant are not uncommon but winds from the north-westerly quadrant are rarely observed. At 500 m, the distribution is markedly different. Although winds from the east and north-east still dominate, other directions are observed with significant frequency. The distribution at 1000 m is similar and at 2000 m a bimodal distribution is observed, with most winds blowing

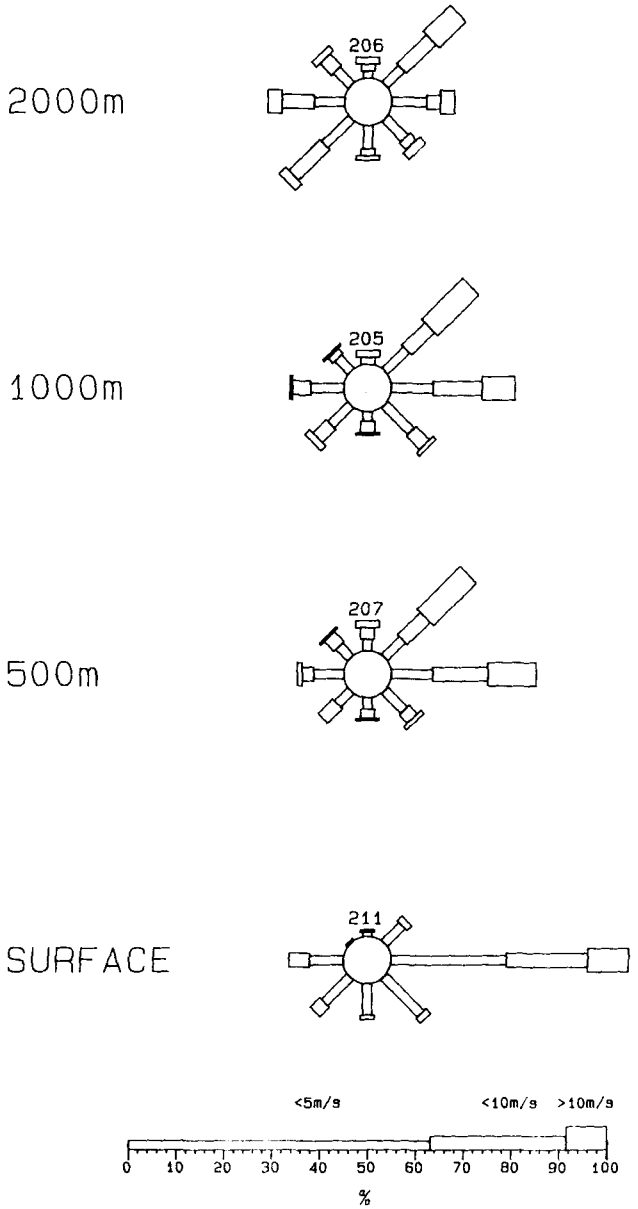


Fig. 4. Wind roses at various levels for Halley, 1985. The number above each rose is the total number of valid observations at that level.

https://doi.org/10.1017/S095410208900026X Published online by Cambridge University Press

from either the north-easterly or south-westerly sectors.

A measure of the directional constancy of the wind is given by

$$D = \left\{\frac{\overline{u}^2+\overline{v}^2}{\overline{u^2+v^2}}\right\}^{\frac{1}{2}} = \frac{\text{Vector mean}}{\text{Scalar mean}} \qquad (1)$$

Table I lists values of D for surface winds at a variety of stations. The value for Halley, $D = 0.55$, is comparable with that for mid-latitude stations and significantly smaller than values for stations in the interior of the continent or for many other coastal regions. The high D-values at these stations are a result of the local topography (Parish 1980); at Halley the local terrain slope is smaller and exerts less of a controlling influence. The directional constancy falls off rapidly with increasing height; $D = 0.45$ at 1000 m and 0.07 at 2000 m.

Table II shows the relative frequency of occurrence of combinations of 2000 m and surface wind directions. Surface winds from the easterly sector are observed with almost all 2000 m wind directions, but are most common with north-easterly winds aloft. A second cluster of observations has

Table I. Directional constancy of the surface wind at selected stations.

	D	Vector mean speed (ms^{-1})	Source
Continental interior			
South Pole	0.79	4.6	Parish (1980)
Vostok	0.81	4.1	Parish (1980)
Mizuho	0.96	11.1	Kikuchi *et al.* (1988)
Continental coast			
Dumont D'Urville	0.91	8.5	Parish (1980)
Cape Dennison	0.97	19.0	Parish (1980)
Davis	0.74	4.6	Parish (1980)
Casey (Wilkes)	0.61	5.7	Parish (1980)
Syowa	0.78	5.8	Parish (1980)
Maudheim	0.60	7.4	Hisdal (1958)
Halley	0.55	7.5	Author
Antarctic Peninsula			
Faraday	0.15	1.1	Author
Rothera	0.49	4.9	Author
Antarctic island			
Signy	0.52	8.8	Author

Table II. Percentage occurrence of surface and 2000 m wind directions in 45° sectors.

		Surface wind sector							
		0	45	90	135	180	225	270	315
2000 m wind sector	0	0.5	0.0	2.4	1.0	0.0	0.5	0.0	0.0
	45	0.0	1.0	15.5	1.9	0.5	1.5	1.0	0.0
	90	0.5	1.0	5.8	3.4	1.5	0.5	0.5	0.0
	135	0.0	1.0	3.9	1.9	1.5	1.5	0.0	0.0
	180	0.0	0.0	2.4	0.5	1.0	1.9	1.5	0.0
	225	0.5	0.0	8.3	2.4	1.5	1.5	4.9	0.0
	270	0.0	2.9	5.8	1.0	0.5	3.4	1.9	0.0
	315	0.5	0.5	5.8	0.5	1.5	0.0	1.0	0.0

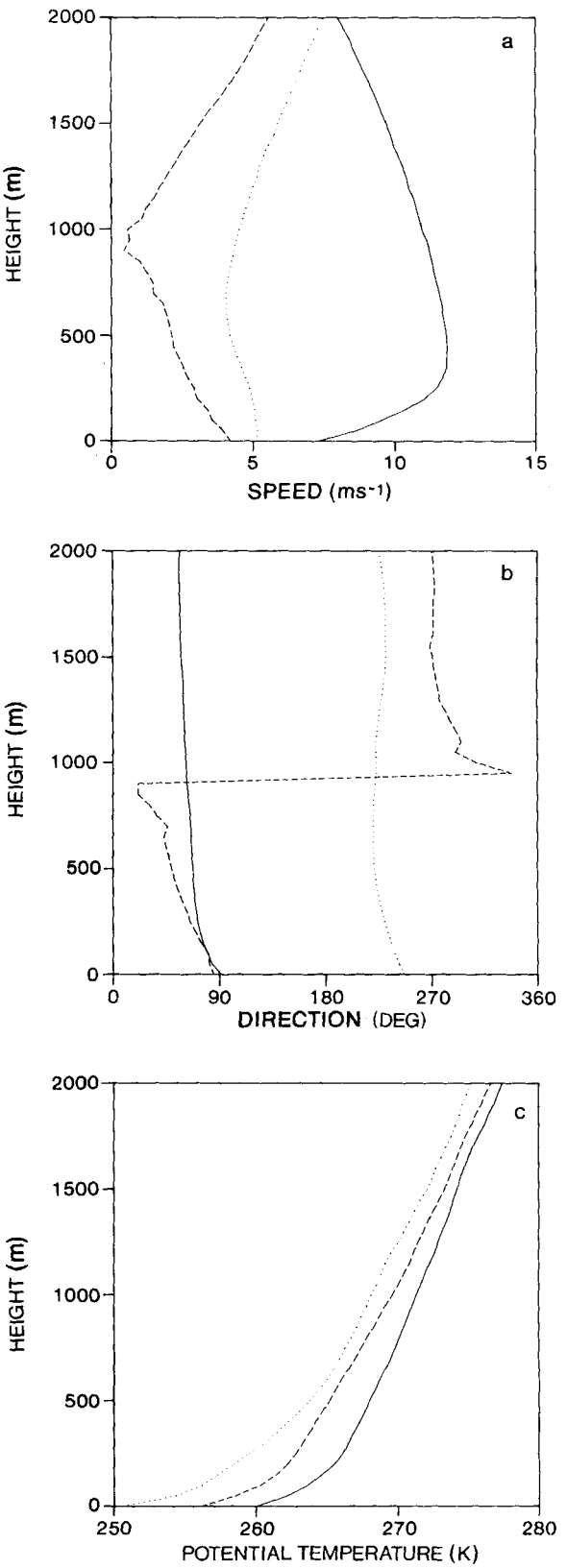


Fig. 5. Composite mean profiles of **a.** wind speed, **b.** wind direction and **c.** potential temperature for the three profile categories discussed in the text. —— = category EE, – – – = category EW, · · · · · = category WW.

https://doi.org/10.1017/S095410208900026X Published online by Cambridge University Press

easterly winds at the surface but westerly or south-westerly winds at 2000 m. Finally, there are a significant number of observations with westerly or south-westerly winds at the surface; in almost all of these cases the 2000 m wind is also westerly or south-westerly. These flow categories will be referred to as 'EE', 'EW' and 'WW' respectively.

Mean wind and potential temperature profiles have been calculated for the three flow categories described above and are shown in Fig. 5. The long averaging period used in the OMEGA wind-finding algorithm has already been mentioned and means that the wind speed and direction profiles (Fig. 5a, b) are based on about four independent pieces of information from each sounding. They are thus a heavily smoothed representation of the 'real' flow.

The mean wind speed profile for the most common flow category, EE, (surface wind from 090° ± 45°, 2000 m wind from 070° ± 45°) has a weak jet profile, with the maximum speed of 11.8 ms^{-1} at about 400 m. The wind direction backs smoothly from 090° at the surface to 060° at 2000 m. When the surface wind is in the same sector but the 2000 m wind is from 270° ± 45°, (category EW) the mean surface wind speed is somewhat less and the wind speed decreases from 4.2 ms^{-1} at 10 m to nearly zero at 1000 m. From 1000 m upwards it increases, reaching 5.5 ms^{-1} at 2000 m. The wind direction backs rapidly from 090° at the surface to about 300° at 1000 m but shows little turning above this height. Individual profiles which fall into this category often exhibit strong shear layers between the low-level easterly and upper westerly flow. It is thought that these may be important regions for internal gravity wave generation (King *et al.* 1987, Rees 1988). When both the surface and 2000 m winds are in the sector 225° ± 45° (category WW) the mean wind speed stays more or less constant at about 5 ms^{-1} up to 800 m, then increases steadily to 7.5 ms^{-1} at 2000 m. The wind direction backs by about 20° between the surface and 2000 m.

Mean potential temperature profiles for the three categories are similar and are shown in Fig. 5c. Above 500 m, the potential temperature gradient shows little variation with height and is about 0.007 K m^{-1} for all categories, corresponding to a Brunt-Väisälä frequency of about 0.015 s^{-1}. Below 500 m, the mean gradient strengthens, indicating the frequent presence of strong surface inversions. It is of interest to note that the lowest near-surface temperatures and strongest low-level stability are observed when the surface wind is from the south-westerly sector.

The climatology of the low-level winds at Halley described above suggests that the near-surface wind is decoupled from the 2000 m wind (and hence the synoptic pressure gradient), and the frequent occurrence of winds from a small range of directions indicates that local topography may exert a large degree of control over the low-level winds. However, the decoupling is not complete and the low-level wind appears to respond to both synoptic and topographic forcing. These factors are considered in the following two sections.

Synoptic forcing

As the Antarctic synoptic observing network is rather sparse, surface pressure distributions have been obtained from analyses supplied by the UK Meteorological Office. These are detailed enough to show the synoptic-scale features which may influence the flow at Halley.

Mean sea level pressure charts for August 1985 were examined in conjunction with the wind profile data from Halley. Easterly sector winds at 2000 m (profile type EE) were generally associated with the passage of a depression from west to east across the Antarctic Peninsula and Weddell Sea. Westerly sector 2000 m winds were seen when there was a high pressure area over the Weddell Sea (centred at about 75°S, 40°W) and also, on some occasions, an area of low pressure centred at about 75°S, 0°W. This latter region is to the north-west of an area identified by Astapenko (1964) as a 'settling' region for cyclones which track southwards into the interior of Antarctica.

During August 1985, the 'travelling depression' synoptic type occurred about twice as frequently as the 'stationary high pressure' pattern. From this limited study, it would appear that the 2000 m wind direction is, at least qualitatively, much the same as the geostrophic wind direction implied by the surface pressure field. The rather low value of directional constancy, D, at 2000 m would appear to be a result of the two most frequently observed synoptic situations giving rise to geostrophic wind directions which are approximately 180° opposed.

When the synoptic pattern is of the 'travelling depression' type, air reaching Halley will have originated round the edge of the Antarctic continent. Stationary high pressure over the Weddell Sea, coupled with low pressure inland, will tend to draw very cold continental air from the Ronne–Filchner Ice Shelf towards Halley. This may explain why lower temperatures are observed when the 2000 m wind is from the westerly sector.

A model of topographic forcing

Description of the model

The dynamics of flows generated when stably-stratified air overlies a sloping surface have been discussed already. Kottmeier (1986) was able to explain the wind regime at Georg von Neumayer station on the Ekström ice shelf using planetary boundary layer resistance laws which incorporated the effects of the baroclinicity caused by the sloped inversion. Here, a simple one-dimensional boundary layer model is used to study a similar problem. This has the advantage that boundary layer wind profiles, not just surface wind speed and direction, are predicted and a reasonably realistic turbulence parameterization can be incorporated. The approach is

https://doi.org/10.1017/S095410208900026X Published online by Cambridge University Press

similar to that of Brost & Wyngaard (1978) but a different turbulence model is used.

The model was originally developed by Mason & Sykes (1982) for initializing a two-dimensional boundary layer model and was modified by King (1985) for studies of the stable boundary layer. It solves the one-dimensional time dependent Boussinesq equations for incompressible flow of a stratified fluid over an infinite, plane of uniform slope γ with an angle ϕ between the fall-line and the x-direction:

$$\frac{\partial u}{\partial t} = fv + \frac{\partial \tau_x}{\partial z} + B \sin\gamma \sin\phi \tag{2}$$

$$\frac{\partial v}{\partial t} = f(u_g - u) + \frac{\partial \tau_y}{\partial z} + B \sin\gamma \cos\phi \tag{3}$$

$$\frac{\partial B}{\partial t} = \frac{\partial H}{\partial z} + \Gamma(B - B_0(z)) \tag{4}$$

The co-ordinate frame is defined so that the geostrophic wind has components $(u_g, 0)$. The synoptic pressure gradient, and hence u_g, is assumed constant with height. $B = g(T - T_0)/T_0$ is the buoyancy, where g is the gravitational acceleration, T the absolute potential temperature and T_0 a reference potential temperature. f is the Coriolis parameter and τ_x, τ_y and H are the turbulent fluxes of momentum and heat respectively. The second term on the right hand side of equation (4) will be discussed below.

Above the boundary layer, the stresses vanish and, in a steady state, the gradients of wind and temperature are simply related through the 'sloped inversion thermal wind' relationship (Parish 1980):

$$-f\frac{\partial v}{\partial z} = \sin\gamma \sin\phi \frac{\partial B}{\partial z} \tag{5}$$

$$f\frac{\partial u}{\partial z} = \sin\gamma \cos\phi \frac{\partial B}{\partial z} \tag{6}$$

The turbulent fluxes are determined by first-order closure, i.e.:

$$\left.\begin{aligned} \tau_x &= \mathrm{K}\,\frac{\partial u}{\partial z} \\ \tau_y &= \mathrm{K}\,\frac{\partial v}{\partial z} \\ H &= \mathrm{K}\,\frac{\partial B}{\partial z} \end{aligned}\right\} \tag{7}$$

and a mixing-length hypothesis is used to calculate the eddy viscosity, K:

$$\mathrm{K} = l^2\left(\left(\frac{\partial u}{\partial z}\right)^2 + \left(\frac{\partial v}{\partial z}\right)^2\right)^{\frac{1}{2}} \tag{8}$$

The mixing length, l, is specified as:

$$\frac{1}{l} = \frac{1}{\kappa z \Phi(Ri)} + \frac{1}{\kappa l_0 \Phi(Ri)} \tag{9}$$

κ is von Karman's constant and Φ is a function of the Richardson number, Ri, defined as:

$$Ri = \frac{\partial B}{\partial z}\left(\left(\frac{\partial u}{\partial z}\right)^2 + \left(\frac{\partial v}{\partial z}\right)^2\right)^{-\frac{1}{2}} \tag{10}$$

If $Ri = 0$ (i.e. no stratification) and $z \ll l_0$, equation (9) reduces to the familiar Prandtl mixing length appropriate to the surface layer. As z becomes large, l will be limited to κl_0. The limiting length scale l_0 is usually assumed to be a fraction of the boundary layer depth (Taylor 1969). King (1985) used $\kappa l_0 = 40$ m and this value is again used here. Recent measurements by the author at Halley suggest that a smaller value of l_0 may be appropriate. However, under conditions of strong static stability, l is largely controlled by the stability function, Φ, and is not very sensitive to the choice of l_0.

The function Φ (Ri) models the damping effect of stable stratification on turbulent transport. Under neutral conditions, $\Phi = 1$ and at some critical Richardson number, Ri_c, turbulence will be suppressed altogether. The simplest functional form for Φ which models this behaviour is:

$$\Phi = \begin{cases} 1 - \dfrac{Ri}{Ri_c} & (Ri < Ri_c) \\ 0 & (Ri \geq Ri_c) \end{cases} \tag{11}$$

Ri_c is set to 0.2 for consistency with the surface-layer similarity forms used to apply the lower boundary condition.

The upper boundary of the model domain is at $z = 3000$ m. Gradients of u, v and B are set to zero, $u = (u_g, 0)$ and $B = 0$ (i.e. the temperature is equal to the reference value, T_0, and the region above 3000 m is assumed to be neutrally stratified). At the lower boundary, a constant buoyancy flux, H_0, is specified. The surface stress, u_*^2, is then determined by iterative solution of the integral form of the surface-layer similarity function for momentum:

$$u(z_1) = \frac{u_*}{\kappa}\left(\ln\left(\frac{z_1}{z_0}\right) + \alpha\frac{z_1}{L}\right) \tag{12}$$

where u is the wind speed at the lowest grid-point, height z_1, z_0 is the roughness length, $L = u_*^3/\kappa H_0$ is the Monin-Obukhov length and α is a constant, set equal to 5 in accordance with measurements (e.g. Webb 1970, Businger *et al.* 1971). Measurements of the roughness length of Antarctic ice shelves by the author and by others (Liljequist 1957, König 1985) suggest that 0.1 mm is an appropriate value for z_0. H_0 is set to 0.001 m^2s^{-3} (roughly equivalent to 30 Wm^{-2}). This is typical of the surface heat fluxes observed at Halley and causes the model to generate a surface inversion of comparable magnitude to those shown on Fig. 5c.

If $H \neq 0$, equations (2)–(4) can only have a steady-state solution ($\partial/\partial t \equiv 0$) if the second term on the RHS of (4) is non-zero. This 'Rayleigh damping' term forces the buoyancy profile, $B(z)$, to return towards a specified profile, $B_0(z)$ with a time constant Γ^{-1}. It is included simply as a device to generate temperature profiles similar to those observed, but may be thought of as representing effects, such as subsidence

https://doi.org/10.1017/S095410208900026X Published online by Cambridge University Press

and advection, which cannot be included in a one-dimensional model, and radiative exchanges, which are not included in this simple model. $B_0(z)$ is chosen to be a linear profile since observed profiles of potential temperature (Fig. 5c) are approximately linear above z = 500 m. The mechanisms which maintain this temperature gradient are not addressed in this study; the temperature field is taken as given and the resultant wind field is modelled.

Equations (2)–(4) are represented in finite-difference form on a stretched mesh, which allows for additional resolution near the surface where gradients are strongest. A steady-state solution is obtained for the zero-slope case ($\gamma = 0$) by matrix inversion and is used as an initial condition. The equations containing the slope terms are then stepped forward in time until a new steady-state solution is reached.

The new equilibrium is achieved through an inertial oscillation about the final state. In the boundary layer this is damped by the eddy stresses, but above the boundary layer it is largely undamped and integration has to proceed for many inertial periods, $2\pi/f$, to reach a steady state. Egger & Schmid (1988) suggest that inertial oscillations in one-dimensional models are often unrealistic; in practice they are damped out by ageostrophic motions which cannot be represented in these models. To save computer time, the following procedure is adopted: the initial solution is first stepped forward for 25 000 s. The solution is then stepped forward for a further $2\pi/f$ s and the profiles are averaged over this time period. The averaged profiles are then used as a new initial condition and the process is repeated until a steady-state is achieved. It has been found that the profiles generated after the first averaging period are within a few percent of the final steady-state and all fields presented here are the result of a single averaging process.

Model results

Before the flow at Halley can be modelled, it is necessary to establish the magnitude and direction of the slope of the ice shelf. Surveys (Thomas 1973) suggest slopes of order 0.001–0.002. Equations (5) and (6) can be used to calculate the slope of isopycnal surfaces from the wind and potential temperature gradients above 500 m shown in Fig. 5. This procedure also yields a slope of about 0.002. The direction of the slope is less easy to establish since survey information is rather incomplete. The Hinge Zone runs approximately NE–SW and the fall line is probably approximately perpendicular to this. In fact, model runs agree best with the observations if the slope is taken as 0.002 and the fall line directed towards 330°.

The model has been used to simulate the three categories of observed mean profiles shown in Fig. 5. Fixed model parameters are summarized in Table III; only the geostrophic wind speed and direction relative to the fall line have been varied. Model wind speed, direction and potential temperature profiles are shown in Fig. 6a–c.

Table III. Parameter values used in the one-dimensional model.

Parameter	Symbol	Value
Surface buoyancy flux	H_0	0.001 m^2s^{-3}
Damping constant	Γ	0.0001 s^{-1}
Background buoyancy	$B_0(z)$	0.0002z–0.6 ms^{-2}
Coriolis parameter	f	−0.00014 s^{-1}
Surface slope	γ	0.002
Roughness length	z_0	0.0001 m
von Karman's constant	κ	0.41
Limiting length scale	l_0	100 m
Critical Richardson number	Ri_c	0.2
Similarity function parameter	α	5.0

The model potential temperature profiles (Fig. 6c) are a reasonable approximation to those observed, but this simply reflects the fact that the background stability, $B_0(z)$, the Rayleigh damping time constant, Γ^{-1}, and surface heat flux have been chosen to achieve this. The conversion from buoyancy to temperature has been made by taking a value of 280 K for the reference temperature, T_0, at a height of 3000 m. The 'surface inversion', or region of enhanced stability close to the surface, is somewhat shallower than observed. This may be due to the absence of radiative effects in the model or is possibly a reflection of the smoothing applied to the radiosonde temperatures by the micro-CORA system.

If the geostrophic wind is set to 5 ms^{-1} from 060°, the modelled wind profile is similar to the observed category EE mean profile. The modelled 10 m wind speed is 8.3 ms^{-1}, slightly greater than the observed mean value of 7.3 ms^{-1}, but the surface wind direction is 090°, exactly as observed. The main differences lie in the structure of the low-level jet. The observed jet is not very sharp and has a maximum of 11.9 ms^{-1} at 400 m. In contrast, the model generates a sharp jet profile with a maximum of 14.3 ms^{-1} at 118 m. Both the model and the observations show the surface wind direction veered by about 30° from the geostrophic direction but in both the turning occurs over the depth of the jet, i.e. over a much shallower layer in the model than in the observations.

When comparing model and observed wind profiles, the averaging applied in deriving winds from the OMEGA signals must be borne in mind. As stated earlier, the observed profiles are smoothed with a 4-min running average and the first 2 min of the profile is simply an interpolation between the surface wind observation and the computed wind at 2 min (approximately 500 m for a normal rate of ascent). If a sharp feature, such as the modelled jet, was present, it would be smoothed out by this procedure. The observations are thus not incompatible with the model results and the sharp low-level jet may actually exist at Halley. Some supporting evidence comes from a limited number of slow ascent rate soundings. These do show a more pronounced jet at a lower level than the category EE

https://doi.org/10.1017/S095410208900026X Published online by Cambridge University Press

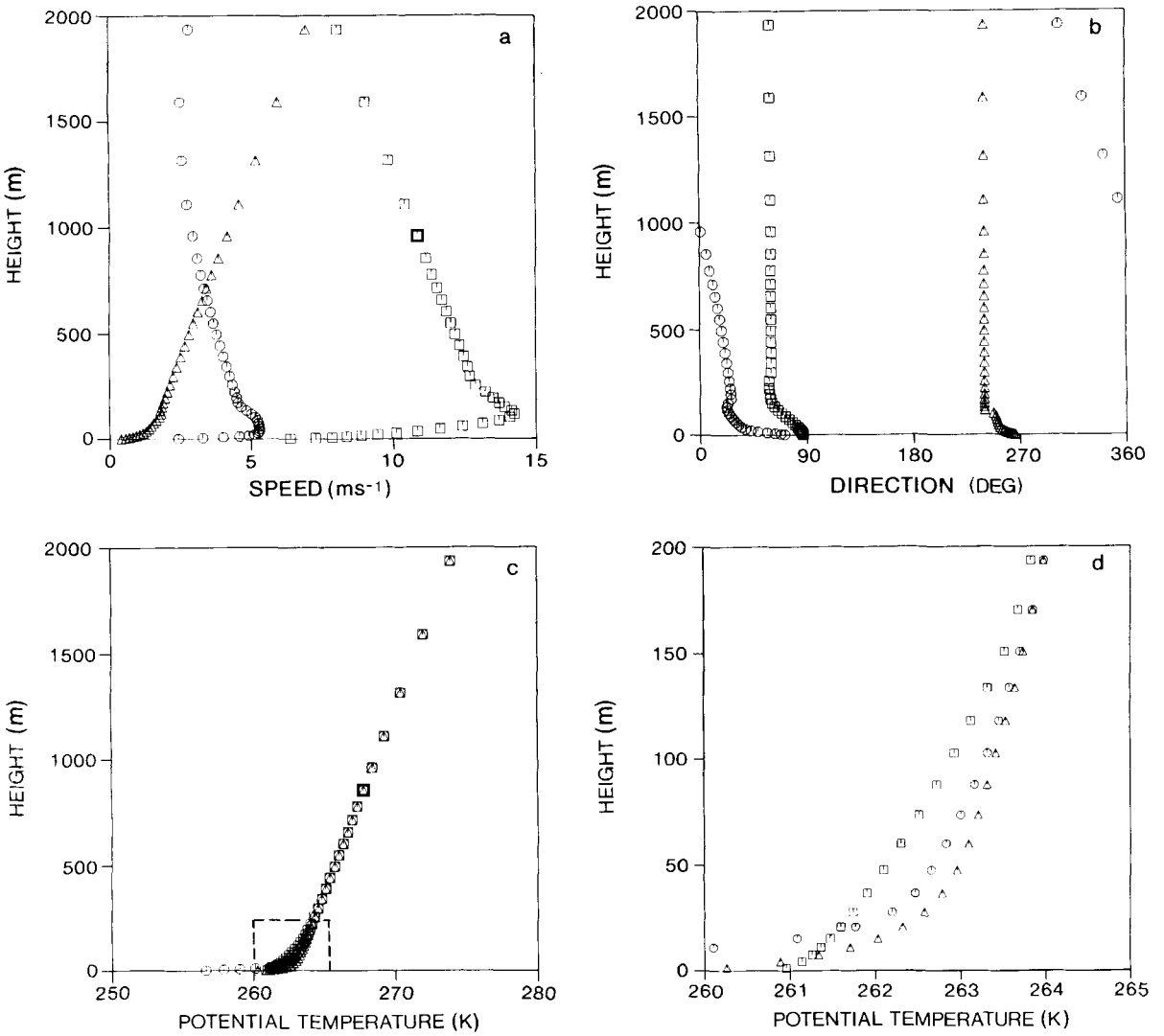


Fig. 6. Model profiles of **a.** wind speed, **b.** wind direction and **c.** potential temperature for three different geostrophic wind velocities. □= 060° 5 ms $^{-1}$, ○ = 270° 5 ms^{-1}, △= 240° 10 ms^{-1}. The detail within the marked area on **c.** is shown on an expanded scale in **d.**

mean profile (Fig. 5a), but further evidence is required from a higher resolution sounding system (possibly a tethersonde or Doppler-Sodar) before the model prediction can be verified.

If the geostrophic wind speed is kept at 5 ms^{-1} , but the direction changed to 270°, the model profiles bear some resemblance to the category EW observed mean profiles. The low-level flow is easterly to north-easterly and the low wind speed (4.6 ms^{-1} at 11 m) reflects the fact that the synoptic pressure gradient and that due to the sloped inversion are now opposed. There is a very shallow low-level jet, with a maximum speed of 5.3 ms^{-1} at 50 m; above this the wind speed declines to a minimum of 2.3 ms^{-1} at about 1600 m and then increases towards the geostrophic value. Above the jet maximum, the wind direction backs fairly uniformly with height. The observed mean profiles for category EW do not exhibit a low-level jet. However, such a shallow feature would almost certainly not be resolved by the soundings. The wind speed is also observed to be reduced to nearly zero at around 1000 m and the change in wind direction from easterly to westerly is concentrated into a shallow layer at around this height.

The category WW profile is simulated by setting the geostrophic wind direction to 240° and its speed to 10 ms^{-1}. The sloped inversion pressure gradient at the surface is now just insufficient to oppose the synoptic pressure gradient and the resultant westerly wind is very weak (less than 1 ms^{-1} at 10 m). The boundary layer is extremely shallow as a result of the low wind speed, the wind direction backing from 266° at the surface to 240° at 118 m. The wind speed increases monotonically with height. This contrasts with the observed mean profile for category WW, which shows an almost constant wind speed up to about 800 m.

The simple 'inversion on a slope' model is thus of help in explaining some of the observed features of the low-level flow at Halley. The wind profiles with north-easterly geostrophic winds are reproduced quite well by the model with

https://doi.org/10.1017/S095410208900026X Published online by Cambridge University Press

the main differences being explained by the poor resolution of the wind-finding system. The relative infrequency of westerly or south-westerly winds at the surface is explained by the fact that a geostrophic wind of greater than 10 ms^{-1} is required to overcome the easterly component forced by the sloped inversion pressure gradient. However, the model is not so successful in reproducing the features of the profiles with westerly geostrophic winds. Although some of the apparent differences may be a result of the poor resolution of the wind soundings, they probably also indicate shortcomings of this simple modelling approach.

With geostrophic winds from the north-easterly sector, the air reaching Halley has had a fetch over the uniform surface of the ice shelf of at least several tens of kilometres. The sloped inversion wind will adjust to a change in slope on a time scale f^{-1}, which corresponds to about 100 km for the wind speeds under consideration. Category EE profiles are thus likely to be in a state of equilibrium with the underlying slope. However, if the wind is from the westerly sector the air reaching Halley will have originated over the Weddell Sea and will have had only a few km fetch over the ice shelf. The flow is thus unlikely to be in equilibrium with the slope of the shelf and the simple one-dimensional model can not be expected to give a good description of the flow.

Conclusions

The low-level flow at Halley appears to be forced both by synoptic-scale pressure gradients and the pressure gradients due to stably-stratified air overlying a sloping surface. The former tend to force geostrophic winds from either a north-easterly or south-westerly direction, while the latter will always act to force an easterly component at the surface. The marked preponderance of easterly surface winds would appear to result from a fortuitous combination of preferred geostrophic wind direction and local terrain slope. A one-dimensional boundary layer model can reproduce the main features of the mean wind profiles when the wind has a long fetch across the uniform ice shelf but is less successful when the wind is blowing on to the ice shelf from the Weddell Sea.

The one-dimensional model is clearly an over-simplification. The ice shelf itself is probably well modelled as a uniformly sloping plane, but slopes which are an order of magnitude steeper exist just inland of the Hinge Zone, only 40 km from Halley. The flow at Halley may thus not be entirely determined by the local slope and advective effects could be important under some circumstances. A further departure from uniformity is the ice front, which is only 10 km from the station. Besides marking an abrupt change in level and gradient the coast may also define a baroclinic zone forced by the difference in temperature between the surfaces of the ice shelf and the sea (or sea ice). It is planned to investigate the two-dimensional structure of the flow by establishing a line of automatic weather stations between the coast and the Hinge Zone. Parish & Waight (1987) have recently applied a two-dimensional boundary layer model to the problem of katabatic flow over a non-uniform slope. Such an approach could profitably be applied to the situation studied here.

Acknowledgements

I would like to thank S.P. Gill for running the upper-air programme at Halley during 1985 and for assembling the dataset used in this study. Surface pressure analyses used in this study were provided by the UK Meteorological Office, which also supports the upper-air sounding programme at Halley.

References

ASTAPENKO, P.D. 1964. *Atmospheric processes in the high latitudes of the Southern Hemisphere.* Jerusalem: Israel Program for Scientific Translations. 286 pp.

BALL, F.K. 1960. Winds on the ice slopes of Antarctica. *In Antarctic meteorology.* London: Pergamon Press, 9–16.

BROST, R.A. & WYNGAARD, J.C. 1978. A model study of the stably-stratified planetary boundary layer. *Journal of the Atmospheric Sciences,* **35**, 1427–1440.

BUSINGER, J.A., WYNGAARD, J.C., IZUMI, Y & BRADLEY, E.F. 1971. Flux-profile relationships in the atmospheric surface layer. *Journal of the Atmospheric Sciences,* **28**, 181–189.

EGGER, J & SCHMID, S. 1988. Elimination of spurious inertial oscillations in boundary-layer models with time-dependent geostrophic winds. *Boundary-Layer Meteorology,* **43**, 393–402.

HISDAL, V. 1958. Surface observations — Wind. *Norwegian-British-Swedish Antarctic Expedition 1949–52. Scientific results,* **1**. Oslo: Norsk Polarinstitut, 67–121.

KIKUCHI, T, AGETA, Y OKUHIRA, F & SHIMATO, T. 1988. Climate and weather at the advance camp in East Queen Maud Land, Antarctica. *Bulletin of Glacier Research,* **6**, 17–25.

KING, J.C. 1985. Modelling the development of large eddies in the stable atmospheric boundary layer. *In* HUNT, J.C.R., *ed. Turbulence and diffusion in stable environments.* Oxford: Oxford University Press. 205–223.

KING, J.C., MOBBS, S.D., DARBY, M.S. & REES, J.M. 1987. Observations of an internal gravity wave in the lower troposphere at Halley, Antarctica. *Boundary-Layer Meteorology,* **39**, 1–13.

KÖNIG, G. 1985. Roughness length of an Antarctic ice shelf. *Polarforschung,* **55**, 27–32.

KOTTMEIER, CH. 1986. The influence of baroclinicity and stability on the wind and temperature conditions at the Georg von Neumayer Antarctic station. *Tellus,* **38A**, 263–276.

LILJEQUIST, G.H. 1957. Energy exchange of an Antarctic snow-field. *Norwegian-British-Swedish Antarctic Expedition 1949–52. Scientific results,* **2**. Oslo: Norsk Polarinstitut, 187–236.

MASON, P.J. & SYKES, R.I. 1982. A two-dimensional numerical study of horizontal roll vortices in an inversion capped planetary boundary layer. *Quarterly Journal of the Royal Meteorological Society,* **108**, 801–823.

PARISH, T.R. 1980. *Surface winds in East Antarctica.* Ph.D Thesis, University of Madison-Wisconsin, 121 pp. [Unpublished.]

PARISH, T.R. & WAIGHT, K.T. 1987. The forcing of Antarctic katabatic winds. *Monthly Weather Review,* **115**, 2214–2226.

REES, J.M. 1988. *Studies of internal gravity waves in the stably stratified*

https://doi.org/10.1017/S095410208900026X Published online by Cambridge University Press

troposphere. Ph.D. thesis, University of Leeds, 303 pp. [Unpublished]

SCHWERDTFEGER, W & MAHRT, L.J. 1970. The relation between the Antarctic temperature inversion in the surface layer and its wind regime. *Proceedings of the International Symposium on Antarctic Glaciological Exploration, Hanover, N.H. Publication no. 86 of the International Association of Scientific Hydrology*, 308–315.

TAYLOR, P.A. 1969. On planetary boundary layer flow under conditions of neutral thermal stability. *Journal of the Atmospheric Sciences*, **26**, 427–431.

THOMAS, R.H. 1973. The dynamics of the Brunt Ice Shelf, Coats Land, Antarctica. *British Antarctic Survey Scientific Reports*, No. 79, 49 pp.

WEBB, E.K. 1970. Profile relationships: the log-linear range and extension to strong stability. *Quarterly Journal of the Royal Meteorological Society*, **96**, 67–90.

https://doi.org/10.1017/S095410208900026X Published online by Cambridge University Press